https://doi.org/10.5194/egusphere-2022-539
Preprint. Discussion started: 29 June 2022

Detecting anomalous sea-level states in North Sea tide gauge data using of autoassociative Neural Network

Kathrin Wahle[1], B. Emil V. Stanev[1,2], Joanna Staneva[1]

[1]Helmholtz Zentrum Hereon, Geesthacht, Germany
[2]University, Sofia, Bulgary

Correspondence to: Kathrin Wahle (kathrin.wahle@hereon.de)

Abstract.

Sea level in the North Sea is densely monitored by tide gauges. These measurements are used for validation as well as for the detection of extreme events. Here, we focus on the detection of sea level states with anomalous spatial correlations. An autoassociative neural network emulates the spatial correlations of gauges in a lower dimensional subspace. Anomalous sea-level states are defined by means of failure of the reconstruction model. Using spatially distributed data as input to the network thus reveals sea-level conditions with unusual spatial correlations. The corresponding atmospheric conditions indicate high wind tendencies and pressure anomalies. Quantitative analysis of such states might help assess and improve numerical model quality in the future as well as provide new insights into the nonlinear processes involved. The method has the advantage of being easily applicable to any tide gauge array without preprocessing the data or acquiring any additional information.

1 Introduction

The dynamics of sea level in tidal basins are one of the most addressed topics in physical oceanography. Theoretical prediction of tidal motion was pioneered by the application of Fourier analysis to tidal motions by Lord Kelvin (Thomson, 1880) and later improved by Doodsen (1921), who developed the tide-generating potential in harmonic form. Analysis and interpretation of tidal observations by Proudman and Doodson (1924) enhanced the understanding of sea-level fluctuations due to winds and changes in atmospheric pressure. The development of numerical 2D storm surge models by Peeck et al., (1983) and Flather and Proctor (1983) led to early warning systems for coastal flooding. With increasing computational power and the availability of satellite data, sea-level predictions have been continuously improved. However, current model predictions are not always perfect and thus emphasize the need to gain further understanding.

A recent important evolution in predicting sea-level in the North Sea was achieved in the framework of the development of the Northwest European Shelf forecasting system (e.g. O'Dea et al., 2012, Tonani et al., 2019).

Regional sea-level variability and trends in the Baltic Sea have been largely studied using tidal gauge measurements. Satellite altimetry has added critical additional information in the last 30 years (Madsen et al., 2015). However, different measurement techniques have different advantages and disadvantages. Satellite-derived sea-level information, which has revolutionized

https://doi.org/10.5194/egusphere-2022-539
Preprint. Discussion started: 29 June 2022

oceanography and climate science, particularly addressing global and large-scale change, is of limited use when addressing near-coastal short-periodic variability. However, advancements are underway, and new satellite missions characterized by better spatial and temporal sampling pave the way for improvements in coastal sea-level research (e.g. Dieng et al., 2021; Prandi et al., 2021; Dodet et al., 2020). In addition, they are not very precise in coastal areas and do not sufficiently resolve the short-periodic variability. What is also currently available is data from operational models, which provide good temporal and spatial coverage. Tidal gauges provide precise estimates with high temporal resolution in specific locations along the coast but do not provide information about the basin-wide patterns of sea level. Furthermore, these data are not continuous; different gauges do not always operate simultaneously; and there are gaps in many of the records. Therefore, a question arises as to whether one can combine data from gauges and independent 2D maps of sea level (from models) to produce a consistent data set (covering all coastal locations at the same time and with high temporal resolution). A similar exercise was undertaken recently by Zhang et al. (2020) for the North Sea and by Madsen et al. (2019) for the Baltic Sea. Tide gauge stations operating along the North Sea coast provide high-quality records of sea level observations over a long period (Wahl et al., 2013). Ponte et al. (2019), reviewing the state-of-the-science of coastal sea-level monitoring and prediction, outlined the importance of sea-level observations for studying sea-level variability.

The North Sea (Figure 1) is a shallow sea with an average depth of ~ 90 m located at the European continental shelf. The dynamics of sea level in the North Sea, which is the region of our present study, can be considered a coupled response to different forcings, such as barotropic tides, wind and atmospheric pressure, as well as forcings from the open boundaries and rivers, including a thermohaline forcing. The coupling of the respective processes is, in most cases, nonlinear, that is, one cannot easily consider the response to individual drivers in isolation. Thus, there is a need to use analytical methods tailored to detect and reproduce nonlinear dynamics. The nonlinear processes are difficult to predict, even with perfect models; therefore, one also has to identify situations in which predictions fail. Furthermore, it is interesting to understand the reasons for the deviation in the model predictions from the observations. The detection of such situations in data from a network of tide gauges is the aim of the present study.

Simple linear statistical methods, such as principal component analysis (PCA), fail to predict nonlinear dynamics because they represent linear combinations of mean states. Flinchem and Jay (2000) demonstrated that wavelet transforms provide an approach, that is well applicable to tidal phenomena that “deviate markedly from an assumed statistical stationarity or exact periodicity inherent in traditional tidal methods”. Wavelet analysis can also reveal features that harmonic analysis could not elucidate.

Here we use autoassociative neural nets (AANNs) as an alternative approach to detect such anomalous sea-level states. Similar to PCA, this method is based on the assumption that the data can be compressed into a lower dimensional subspace. The combination of nonlinear components best describing the variability in the training data can be used to reconstruct the data themselves. Subsequently, data with correlations similar to those of the training are reproduced well.

AANN provides such a nonlinear reconstruction model, with the reconstruction error as a measure of how well data are characterized by the model. Large errors in the reconstruction of independent data by the model signals situations, in which

https://doi.org/10.5194/egusphere-2022-539
Preprint. Discussion started: 29 June 2022

data do not belong to the same distribution the model was built on. For sea-level, the entirety of tide gauge measurements in the North Sea will show specific spatial correlations (changing in time with the tide). However, in anomalous situations (e.g. localized storms) these correlations may drastically change. In this context, neural networks have been used for (extreme) tidal surge prediction (French 2017, Tayel 2015, and Bruneau 2020). Similarly, Hieronymus et al. (2019) applied different machine learning techniques to the regression problem of time series tide gauge data, and Balogun and Adebisi (2021) investigated the impact of different ocean-atmosphere interactions on sea-level predictability using different NNss. However, all these applications are limited to single tide gauge stations.

Horsburgh (2007) proved the importance of spatial and temporal correlations among tide gauge stations along the British coast for the distribution of surge residuals. However, their linear model is only capable of describing some of the possible interactions between tides and surges and was used to demonstrate the existence of critical spatiotemporal scales for surge development and decay. Wenzel (2010) used Neural Networks for the reconstruction of monthly regional mean sea-level anomalies from 59 tide gauges worldwide. Zhang et al. (2020) used generative adversal networks to reconstruct the sea level in the North Sea from an array of coastal tide gauge data. Similarly, Yang et al. (2021) used deep learning to fuse altimeters data with tide gauge data in the Mediterranean Sea. Nieves (2021) et al. used open ocean temperature to predict coastal sea level variability.

In contrast to all these applications, we will focus on the opposite: we will analyse data from an array of tide gauges in the North Sea simultaneously to identify situations in which their spatial correlations deviate greatly from the mean correlations. Atmospheric conditions related to such situations might aid further understanding and future developments in sea-level prediction.

The paper is structured as follows. In section 2 we present the method and data used. Section 3 presents the extreme events and their relationship with the atmospheric conditions, followed by a discussion and conclusions

2. Methods

The spatial and temporal correlations of tide gauge data mirror the complex sea-level dynamics in the North Sea, originating from the interactions among different forcings. First, the propagation of the tidal wave is influenced by North Sea topography. The north-south decline of water depth shifts the central amphidromic point southwards (see Figure 1a for the oscillation pattern of the semidiurnal M2 tide). Two additional amphidromies are generated as a result of a superposition of incident and reflected Kelvin waves and cross-shore Poincare waves with centres in the north off the Norwegian coast, and in the south between Suffolk and Holland (Figure 1a). The amplitude of the tidal wave increases towards the British coast. Off the Danish and Norwegian coasts amplitudes are significantly smaller due to dissipation by bottom friction in the shallow southern part of the North Sea.

https://doi.org/10.5194/egusphere-2022-539
Preprint. Discussion started: 29 June 2022

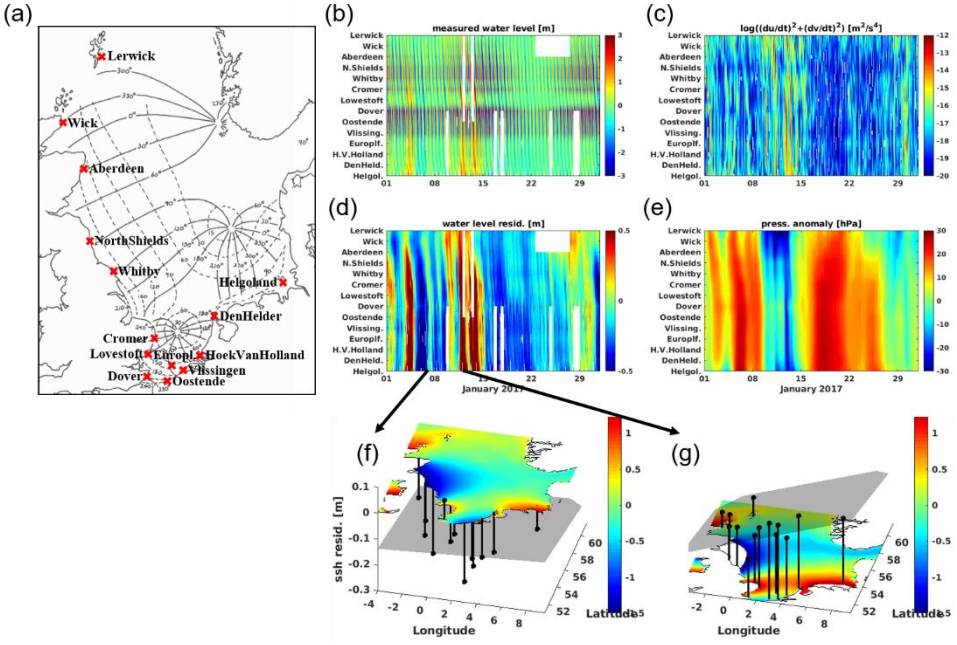

Figure 1: (a) Location of tide gauge stations used in this study and M2 cotidal chart. (b-d) Time series of measured water levels, water level residuals, wind tendency and pressure anomaly for January 2017 at tide gauge positions. (f, g) Snapshots of NEMO model water levels for two selected timepoints. Black bars show water level residuals at tide gauge locations together with a plane fitted linearly to these residuals (grey areas).

Second, the circulation of the North Sea and thus the sea level is forced by the atmosphere through the vertical flux of momentum due to either wind stresses or atmospheric pressure gradients. Considering the length scales and depth of the North Sea, the wind will have a dominant effect. The prevailing westerly winds result in a dominant cyclonic circulation, and reversed rotation (easterly winds) seldom occurs. For northwesterly and southeasterly winds, circulation might stagnate. As shown by Jacob et al. (2017), the interaction of tidal and wind-driven currents becomes nonlinear in areas of strong currents, particularly in the German Bight. They also demonstrated that the ocean response to atmospheric variability does not mimic that one, and the atmospheric variability affects the spring-neap variability more strongly than the M2 tide.

In summary, the specific topography of the North Sea together with nonlinear effects lead to complex circulation patterns that hamper sea level prediction.

2.1 Observational and Model Data

Observational sea level data along the North Sea coast have been obtained from the Copernicus - Marine environment monitoring service (CMEMS, http://marine.copernicus.eu/). Altogether 14 gauge stations with hourly data are used. Their positions are shown in Figure 1a. Figures 1b and d show the time series of measured and detided (residual) water levels. The

https://doi.org/10.5194/egusphere-2022-539
Preprint. Discussion started: 29 June 2022

former show the propagation of the tidal wave along the English coast (with water levels increasing southward towards the channel), whereas the latter ones resemble the atmospheric forcing (Figure 1c, e). In the presence of large gradients in wind tendency (Figure 1g), the water surface tilts considerably.

For the experiments discussed later in this study, we use only the ocean circulation part based on the Nucleus for European Modelling of the Ocean (NEMO v3.6; Madec, 2017, Staneva et al., 2017, 2021, Bonaduce et al., 2020) with 3.5 km horizontal resolution as an ocean component of the Geesthacht Coupled cOAstal model SysTem (GCOAST). The NEMO setup used within the GCOAST system has an eddy-resolving spatial resolution of ~3.5 km, and uses an explicit free-surface formulation (Madec 2017; Staneva et al. 2021, Bonaduce et al., 2020). The model area covers the Baltic Sea, the Danish Straits, the North Sea and part of the northeast Atlantic Ocean. The data used in the present study are only for the region shown in Figure 1. The vertical discretisation of the NEMO se-up uses 50 hybrid s-z* levels with partial cells. Atmospheric pressure and tidal potential are also included in the model forcings (Egbert and Erofeeva, 2002). Daily river run-off is based on river discharge dat asets from the German Federal Maritime and Hydrographic Agency (Bundesamt für Seeschifffahrt und Hydrographie, BSH), Swedish Meteorological and Hydrological Institute (SMHI) and United Kingdom Meteorological Office (Met Office). Boundary conditions at the open boundaries are taken from the AMM7 model (O'Dea et al., 2012) distributed by the Copernicus Marine Environment and Monitoring Service. The model forcing for momentum, and heat fluxes are considered using bulk aerodynamic formulae, and hourly data from atmospheric reanalyses of the European Centre for Medium Range Weather Forecasts (ERA5, Hersbach et al, 2020), the 5th generation of reanalysis of the ECMWF. ERA5 has horizontal resolutions of 28 km and 31 km, respectively. We used ERA5 1-hourly products provided by Copernicus Climate Center Service (C3S, 2021) available with 0.25° and 0.25° horizontal resolutions for the atmospheric and wave parameters, respectively. Several studies have demonstrated the advantages of using ERA5 over its predecessor (ERA-INTERIM, e.g. Belmonte Rivas and Stoffelen, 2019).

2.2 Autoassociative neural net

Most environmental monitoring programs produce large sets of multivariate data, with the tide gauge data network in the North Sea being among them. These multivariate data are determined by a number of factors (here tidal and atmospheric forcing, together with bathymetry, river input, etc.) and hence can be considered to be generated from them. Since the number of factors is often smaller than the number of observed variables, the data are located within a subspace of the given data space. This subspace can be described by its (linear or nonlinear) components. The components serve to construct a model, with the reconstruction error as a measure of how well data are characterized by this proxy. Thus, large reconstruction errors signal anomalous situations in the sense that data are not located in the spanned subspace. The model aims to provide a tight enclosure of the subspace spanned by the data under normal conditions. Here, anomalous applies to data not lying within the bounds of this model and not belonging to the same distribution the model was built on. Due to the absence of an appropriate model of

https://doi.org/10.5194/egusphere-2022-539
Preprint. Discussion started: 29 June 2022

the underlying processes, it is very often difficult to detect such situations hidden in the data. In many such cases, autoassociative neural nets could be the proper tool to use to become aware of these situations.

An AANN is a reconstruction model based on feed-forward neural net (Kramer 1992). It maps the **n**-dimensional input **x** onto itself (**x'**) with a data compression step in between: The number of neurons in at least one hidden layer in an AANN is less than the dimension **n** of the input and output vectors **x** and **x'**. This layer is called the bottleneck-layer and is the key component of an AANN (Figure 2a). It provides data compression of the input with powerful feature extraction capabilities. The mapping part m(**x**) compresses the information of the **n**-dimensional vector to a smaller dimension subspace vector **p**, whereas the demapping part **x'**=d(**p**) uses compressed information to regenerate the original **n**-dimensional vector.

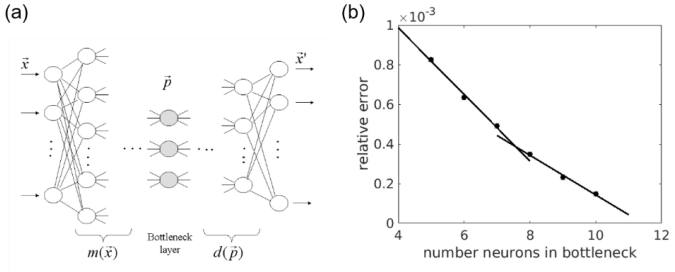

Figure 2: (a) Autoassociative NN with bottleneck: the input is mapped by p = m(x) onto a lower dimensional space (dim(p)<dim(x)) and is approximately reconstructed by the demapping NN part x' = d(p) ≈ x. (b) Error measure from the training sample versus the number of neurons in the AANN 'bottleneck'–layer using the 2016/17 North Sea water level data from 14 tide gauge stations.

Thus, the mapping part takes advantage of the (nonlinear) correlations/functional relations existing among the input variables (here, the spatial correlations). Thus, an AANN can be considered to perform a nonlinear generalization of the Principal Component Analysis (Nonlinear Principal Component Analysis, NLPCA (Kramer 1991)). Similar to PCA, NLPCA can also serve important purposes, e.g. filtering noisy data, feature extraction, data compression, outliers and novelty detection (Mori 2016).

During training, the AANN constructs a model, that captures the distribution of a given data set. This model shows that the intrinsic dimensionality (= the number of independent components) of the data set is not higher than the number of neurons in the bottleneck layer.

Thus, an important step in the construction of an appropriate AANN is the choice of the number of neurons in the bottleneck layer, i.e., to determine the dimension of the subspace **p**. The choice is based on the reconstruction abilities of the network: The overall reconstruction error of the AANN decreases with an increasing number of neurons in the bottleneck layer. However, if the number of bottleneck neurons equals the intrinsic dimensionality, a further increase leads to 'overfitting' of the AANN, i.e., learning stochastic variations in the data set rather than the underlying functions. As a result, the decrease in the overall error flattens (see Figure 2b).

https://doi.org/10.5194/egusphere-2022-539
Preprint. Discussion started: 29 June 2022

2.3 Application of AANN to the North Sea water level from tide gauges

The proposed scheme was applied to data from 14 (dim(**n**)=14) tide gauges along the North Sea coast (see section 2.1). The data set was used to train the AANNs spanning 2016 and 2017. Data from 2018 were kept as an independent testing set. The two-year period is assumed to be long enough to capture the essential spatial correlations among observations at different gauges well. Thus, any dominant factor affecting the interrelationship between observations from individual stations, (bathymetry, the distance between stations, dominant winds and atmospheric pressure, etc.) should be reflected by the AANN. The choice of tide gauge locations was a compromise between spatial coverage and data availability (since missing data from single gauge stations were not filled, e.g., by interpolation and thus resulted in data loss).

A sequence of AANNs with an increasing number of neurons in the bottleneck layer was trained to map the 14 water levels onto themselves. In Figure 2b the relative reconstruction error **e** for all training data is plotted versus the number of neurons in the bottleneck layer. As expected, the error decreases with an increasing number of bottleneck neurons. Two different regimes are visible: one regime is for the number of bottleneck neurons below approximately seven and the other regime is for those above this number. Therefore, the smallest AANN belonging to the second regime with seven neurons (dim(**p**)=7) in the bottleneck layer is chosen.

2.4 Quality of AANN analysis

The performance of the AANN is shown in Figure 3. The scatterplots compare the modelled vs. observed sea-level data. The distribution for the training phase (Figure 3a) closely follows the bisectrix and is very narrow. The standard deviation between the observed and modelled data is well below 1 cm (Figure 3e). During the validation phase (Figure 3b, f), the agreement between the observations and modelled data is almost as good as that for the training phase; however, some scatter is also clearly seen. Parts of this disagreement, with errors above the 99.9 percentile during the training phase, are marked red and indicate possible candidates for anomalous situations, which will be further analysed. The distribution of errors is non-Gaussian during training and testing (Fig. 3e,f). The long tail of the error histogram presents data where the reconstruction by AANN failed and where anomalous correlations among tide gauges are expected.

The non-Gaussian nature of the error distribution demonstrates the capability of the AANN to capture complex (usually nonlinear) processes. This is the fundamental difference from the case when PCA (with the same subspace dimension) is used to reconstruct the observed data (Figure 3 c, d and g, h). The latter model shows errors, which are two orders of magnitude larger than the errors in the AANN reconstruction, indicating non-linearity of the underlying physics. In this case, the linear statistical model leads to a short-tailed Gaussian error distribution (Figure 3g, h), making it unsuitable for the desired task.

https://doi.org/10.5194/egusphere-2022-539
Preprint. Discussion started: 29 June 2022

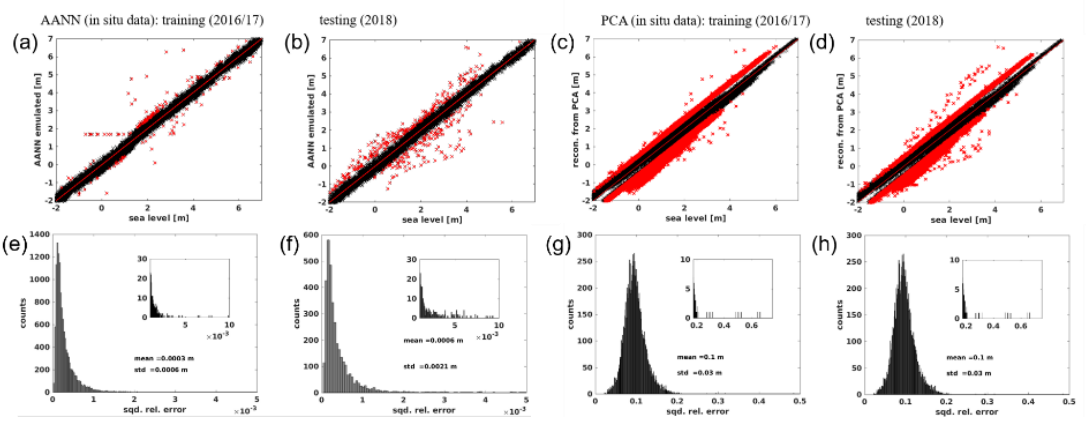

Figure 3: Performance of the AANN and PCA in reconstructing sea-level data. (a-d) Scatterplots of measured vs. modelled sea-level data for the training period (a, c) and testing period (b, d). Points reconstructed with an error 99.9% above of all others during training of the AANN are plotted in red in either case. Histograms (e-h) show the respective distributions of squared relative reconstruction errors. The numbers are the mean error and standard deviation of the reconstruction. The insets represent the tail of large errors, which are possible candidates for anomalous sea states.

3. Anomalous sea-levels and their relationship with the atmospheric conditions

To isolate events that strongly affect the spatial correlations among several tide gauges, further constraints are needed. High values of AANN reconstruction errors might originate from events on small scales, such as ocean response to wind gusts, as well as the erroneous measurement of a single tide gauge. Thus, we postulate that a given threshold error has to be exceeded by at least 3 gauges for at least 3 hours.

To exclude the dependence of identification of such extreme events from the data used, we trained the AANN based on the following three data sets:

- trained with data extracted at the closest positions of gauge stations from the CMEMS operational model AMM15 (AANN_NEMO);
- trained with data from only 10 stations (with Dover, Oostende, Vlissingen and Europlatform in the southwest corner of the North Sea excluded) (AANN_less); and
- trained with detided data from the 14 gauge stations (AANN_resid).

The first additional network AANN_NEMO allows an intercomparison between observations and simulations. If the agreement is good, areal coverage of data from the operational model will enable the analysis of horizontal patterns associated with the identified events. The second network AANN_less identifies the possible occurrence of such events in the southwest North Sea area, which is characterized by its complex dynamics and high amplitudes of tidal oscillations. This area is known

https://doi.org/10.5194/egusphere-2022-539
Preprint. Discussion started: 29 June 2022

to be dominated by a small amphydrome (Fig. 1a). The third network AANN_resid reveals how strongly anomalous events are associated with the basic tidal dynamics, which are removed from the training and control data sets.

The error distributions of AANN_less and AANN_resid resemble those of the reference AANN, whereas the tail of the AANN_NEMO error distribution is shortened, making it less suitable for novelty detection (see Figure 4a,b,d,e). A plausible explanation is that model physics is constrained to Gaussian processes and is by definition consistent, whereas observational data have errors. This hypothesis is confirmed by a comparison of measured, NEMO modelled and AANN emulated water level residuals (Figure 4c). Generally, the three are in good agreement with each other, but an exceptionally high residual at station Cromer around June 7th is not reproduced by the NEMO model and would thus result in a large reconstruction error.

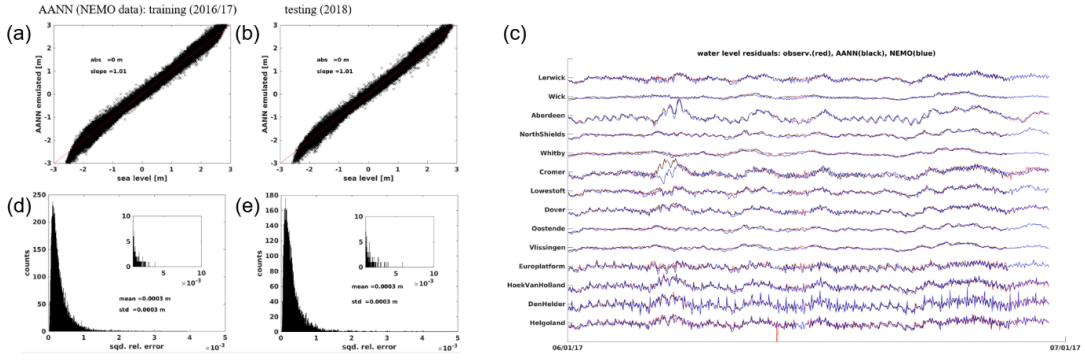

Figure 4: (a,b,d,e) Same as Fig. 3 but for AANN_NEMO trained on NEMO modeled sea level data. (c) Time series of water level residuals at the 14 tide gauge locations as observed (red lines), as emulated by AANN (black lines) and as modeled by NEMO (blue lines) for June 2017.

Table 1: Overview of the number of events detected by alternative approaches, based on anomalous sea states identified in the reference model during the validation period.

	Spring (MAM)	Summer (JJA)	Autumn (SON)	Winter (DJF)
AANN_NEMO	2	2	6	13
AANN_less	1	0	6	13
AANN_resid	1	1	6	13
AANN	**2**	**2**	**6**	**13**

The proposed criterion was tested on the reference model for the validation period. Several anomalous sea states were detected (Table 1). Events in the winter months occur more than twice as often as in other seasons. Afterwards, it was verified whether a specific event could be observed with the alternative approaches (see Table 1). Due to the short-tailed error distribution, all

https://doi.org/10.5194/egusphere-2022-539
Preprint. Discussion started: 29 June 2022

235 events can be detected with AANN_NEMO (but as a stand-alone method, it gives a large number of false alarms). Events from autumn and winter are also detected with the alternative AANNs (AANN_resid and AANN_less), which differs for spring and summer, where some events are not detected with AANN_less and/or by AANN_resid.

In the following section, we will analyse two such events:

240 The first event from June 2017 (low pressure 'Heinrich') was chosen since it was detected by AANN_resid but not by AANN_less (Figure 5 a, b and d, e). This system brought some unseasonably wet and windy weather from France to the British southeast coast. The rain was accompanied by very strong westerly winds (~15 m/s), with gusts of 20–25 m/s around the coast of England and Wales (see the snapshot in Figure 5). As a result, the measured sea-level exceeded the modelled sea-level over several hours along the western Dutch coast and southeastern British coast. AANN model error is the largest at Oostende,

245 where the measured low tide is higher than the low tide expected by AANN (Figure 9a upper panel). The NEMO model error is largest for Lowestoft, where it underestimates the measured values for both high and low tides (Figure 9a lower panel). Thus, the forcing resulted in a localized (exceptional) increase in sea level. The snapshot of NEMO water levels visualizes this finding in Figure 5 at the time the AANN largest errors occurred. The water level residuals at tide gauge stations confirm this result (see inclination angle of plane fitted to residuals).

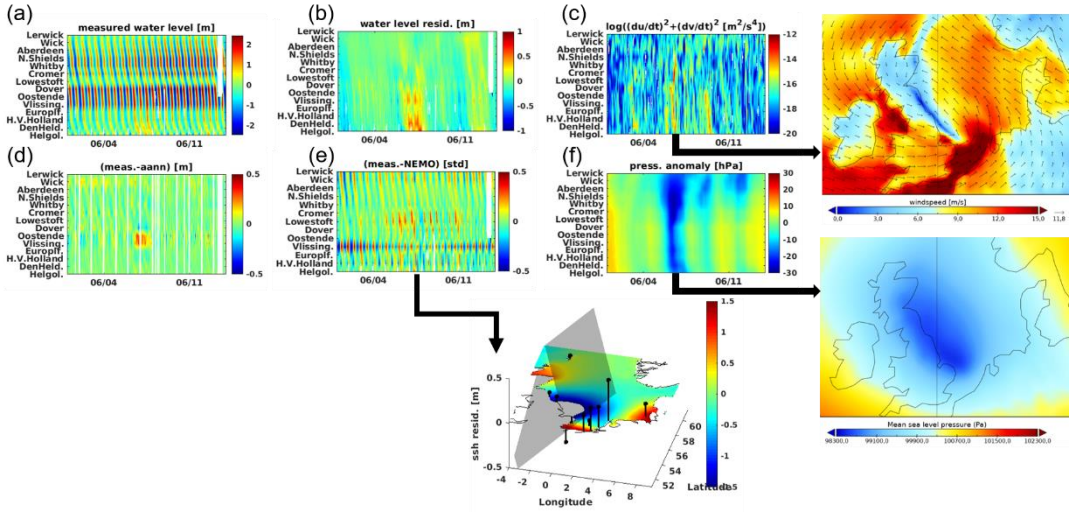

Figure 5: Hovmoeller diagrams of measured tide gauge data (a), its residuals (b) and atmospheric forcing (ERA 5 data, wind tendency (c) and pressure anomaly (f)) for 14 stations along the inner North Sea coast for an ~14-day period in June 2017. The snapshots show the wind and pressure field at the time of the largest wind tendency occurrence. The AANN reconstruction error is given in (d), where the period within the criteria for anomalous sea state distributions are met, is highlighted. (e) shows the NEMO model error. Relatedly, the snapshot shows NEMO ssh at the time of largest AANN error together with tide gauge residuals (bars). The grey area shows the orientation of a plane fitted linearly to these residuals.

250

https://doi.org/10.5194/egusphere-2022-539
Preprint. Discussion started: 29 June 2022

AANN_resid (Figure 6b) also found the event. Even though residuals are largest at DenHelder, AANN_resid is still largest for Oostende. However, without the stations around the first amphidrome (i.e., without Dover, Oostende, Europlatform and Vlissingen) AANN_less (Figure 6c) could not detect the event.

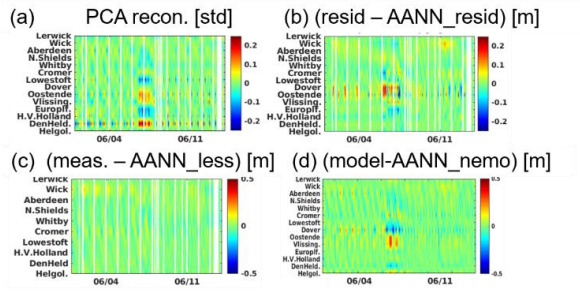

Figure 6: Hovmoeller diagrams of different model reconstruction errors compared to measured (detided) tide gauge data (stations and time period are the same as those in Figure 5): (a) PCA, (b) AANN_resid (trained on water level residuals), (c) AANN_less (without 4 stations close to the first amphidrome) and (d) reconstruction error of AANN_nemo (trained on modelled data) compared to NEMO data.

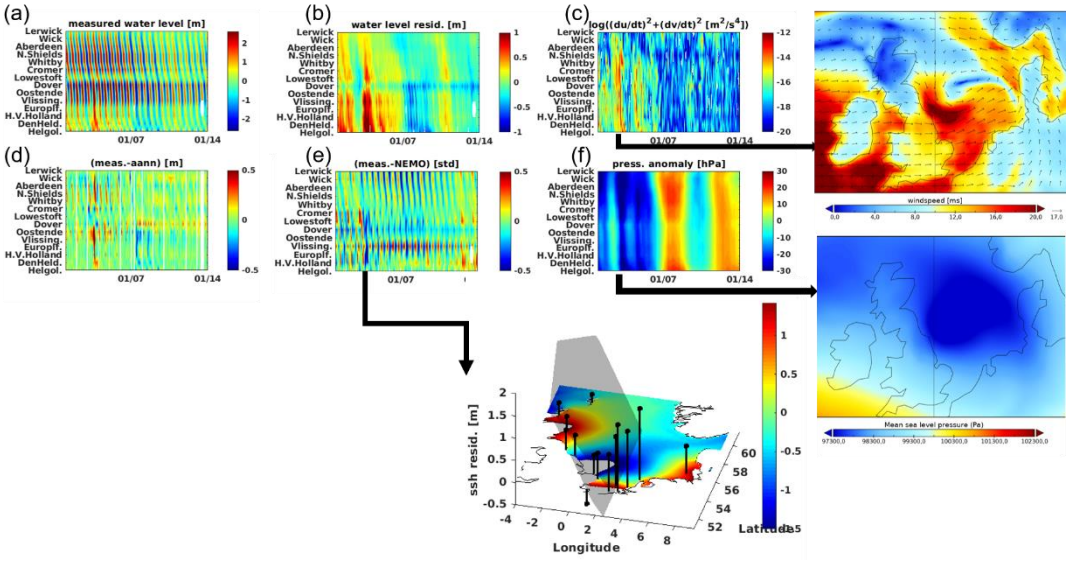

Figure 7: Same as Figure 5, but for January 2018 during storm 'Burglind'.

As a second example, a typical winter storm was chosen: the deep depression 'Burglind' (Figure 7) which was associated with high wind speeds (up to 20 m/s) along the English and the Dutch coasts but also with large gradients in the wind field (Figure 7c) with gusts exceeding 33 m/s in England and Wales. The storm track passed over Ireland, crossed the United Kingdom and then moved over Central Europe and dissipated.

https://doi.org/10.5194/egusphere-2022-539
Preprint. Discussion started: 29 June 2022

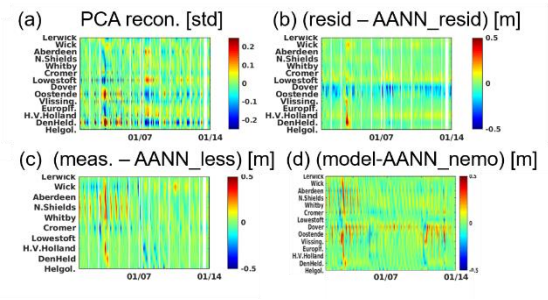

Figure 8: Same as Figure 6, but for January 2018 during storm 'Burglind'.

As a result, the measured tide gauge values exceeded the AANN modelled values at stations along the southern English and Dutch coasts. An exception is Lowestoft in the 'shadow' of the cyclone. The NEMO model results show good agreement during high tide, especially along the Scottish coast (Figure 9b, upper panel), but tend to overestimate the low tide values, especially along the Dutch coast (Figure 7e and 9b, lower panels).

This event also manifests in the error measures of AANN_less (Figure 8c) since the event affects all stations along the English coast (not only the area around the first amphidrome). AANN_resid (Figure 8b) also detects the event. However, here, stations along the Dutch coast have the largest reconstruction errors (i.e., stations with the highest water level residuals, see Figure 7b).

To complete the analyses, Figures 6a and 8a show the PCA reconstruction error for the two time periods. The two events can be clearly identified. However, due to the Gaussian error distribution, PCA model reconstruction with only leading modes will result in high rates of false alarm.

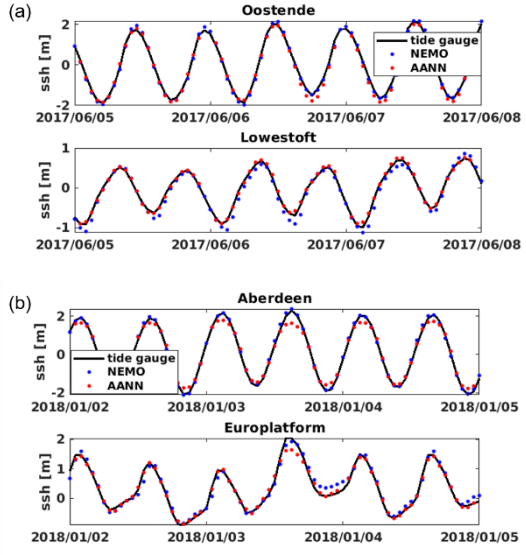

Figure 9: Time series of sea surface height during a four-day period around the two events in June 2017 (a) and January 2018 (b) as measured in situ and as modelled by the NEMO and AANN. The two tide gauges were chosen to represent the model variability (large errors in AANN, small errors in NEMO and vice versa).

https://doi.org/10.5194/egusphere-2022-539
Preprint. Discussion started: 29 June 2022

On either occasion, a typical time delay of 5 to 15 hours between large tendencies in wind forcing and large reconstruction errors are observed, supporting the assumption of the atmosphere plays the key role in the detected events. However, their occurrence cannot be directly linked to atmospheric variables, such as large tendencies in the wind forcing. These tendencies occur often but seldom result in such exceptional sea-level states (see Figures 5c and 7c), where the water surface is unusually tilted.

Conclusions

We presented a tool for detecting anomalous water levels from a network of tide gauges in the North Sea by means of AANN. Strong spatial correlations between gauges allow for a reconstruction model in a lower dimensional subspace. Combining a threshold value for reconstruction error with the requirement of its occurrence at three different gauges for at least three hours has been shown to be a valuable filter for such events. For the two events discussed in detail, atmospheric conditions showed high wind tendencies and pressure anomalies, with the piling up of water masses in specific areas. Thus, the resultant sea states are assumed to be related to nonlinear interactions among the various atmospheric and oceanic forcings. Further analysis is needed to reveal a deeper understanding of the underlying processes. Ultimately, this understanding might improve numerical sea-level predictions. The AANN reveals an intrinsic dimensionality of **p**=7. Evident variable candidates that could be involved in further studies include location (latitude/longitude), time, wind tendency, pressure anomaly and information on water currents.

Otherwise, the tool offers an inexpensive opportunity to monitor the tidal gauge array. The difference between using raw and detided data as input to the model was marginal. Thus, no further data preprocessing is needed. The AANN model reacts sensitively on the choice of tide gauge locations: AANN_less (where stations around the first amphidrome were removed from the training data) was not able to identify events resulting from storms along the channel.

Considering the linear PCA reconstruction method reveals a high rate of false positive alarms because the underlying physics is nonlinear. For similar reasons the detection of some of these events might fail for AANN_NEMO: the fundamental data are consistent throughout space and time and model physics is mainly restricted to Gaussian processes. On the other hand, this finding substantiates the hypothesis, that AANN is able to detect situations under which model physics need further improvement.

The proposed method can be adapted easily to any tide gauge array. However, the intrinsic dimensionality of the constructed AANN might differ as well as the involved variables and underlying processes.

https://doi.org/10.5194/egusphere-2022-539
Preprint. Discussion started: 29 June 2022

*Competing interests***.** The contact author has declared that neither they nor their co-authors have any competing interests.

Disclaimer. Publisher's note: Copernicus Publications remains neutral with regard to jurisdictional claims in published maps and 10 institutional affiliations.

Acknowledgements. We acknowledge the Cluster of Excellence EXC20 2037 "Climate, Climatic Change, and Society" (CLICCS) (project no. 390683824). ES acknowledges the EU H2020 project DOORS (grant no. 101000518). JS acknowledges the European Green Deal project "Large scale RESToration of COASTal ecosystems through rivers to sea connectivity" (REST-COAST) (grant no. 101037097). KW gratefully acknowledges funding from the EU H2020 project IMMERSE (grant no. 821926).

Financial support: This research has been supported by the European Green Deal project "Large scale RESToration of COASTal ecosystems through rivers to sea connectivity" (REST COAST) (grant no. 101037097) and the EU H2020 project IMMERSE (grant no. 821926).

https://doi.org/10.5194/egusphere-2022-539
Preprint. Discussion started: 29 June 2022

References

Balogun, A. L., and Adebisi, N.: Sea level prediction using ARIMA, SVR and LSTM neural network: assessing the impact of ensemble Ocean-Atmospheric processes on models' accuracy. Geomatics, Natural Hazards and Risk, 12(1), 653-674, 2021.

Belmonte Rivas, M., and Stoffelen, A.: Characterizing ERA-Interim and ERA5 surface wind biases using ASCAT. Ocean Science, 15(3), 831-852, 2019.

Bonaduce, A., Staneva, J., Grayek, S., Bidlot, J. R., and Breivik, Ø.: Sea-state contributions to sea-level variability in the European Seas. Ocean Dynamics, 70(12), 1547-1569, 2020.

Bruneau, N., Polton, J., Williams, J., & Holt, J.: Estimation of global coastal sea level extremes using neural networks. Environmental Research Letters, 15(7), 074030, 2020.

C3S: Copernicus Climate Change Service (2021). Climate Data Store (CDS), date of access: https://cds.climate.copernicus.eu/cdsapp#!/home

Dieng, H. B., Cazenave, A., Gouzenes, Y., and Sow, B. A.: Trends and inter-annual variability of altimetry-based coastal sea level in the Mediterranean Sea: Comparison with tide gauges and models. Advances in Space Research, 68(8), 3279-3290, 2021.

Dodet, G., Piolle, J. F., Quilfen, Y., Abdalla, S., Accensi, M., Ardhuin, F., ... and Donlon, C.: The Sea State CCI dataset v1: towards a sea state climate data record based on satellite observations. Earth System Science Data, 12(3), 1929-1951, (2020).

Doodson, A. T.: The harmonic development of the tide-generating potential. Proceedings of the Royal Society of London. Series A, Containing Papers of a Mathematical and Physical Character, 100(704), 305-329, 1921.

Egbert, G. D., and Erofeeva, S. Y.: Efficient inverse modeling of barotropic ocean tides. Journal of Atmospheric and Oceanic technology, 19(2), 183-204, 2002.

Flather, R. A., & Proctor, R.: Prediction of North Sea storm surges using numerical models: Recent developments in UK. North Sea Dynamics, 299-317, 1983.

Flinchem, E. P. and Jay, D. A.: An Introduction to Wavelet Transform Tidal Analysis Methods. Estuarine, Coastal and Shelf Science,51, 177–200 doi:10.1006/ecss.2000.0586, 2000.

https://doi.org/10.5194/egusphere-2022-539
Preprint. Discussion started: 29 June 2022

French J., Mawdsley, R., Fujiyama, T., and Achuthan, K.: Combining machine learning with computational hydrodynamics for prediction of tidal surge inundation at estuarine ports. Procedia IUTAM, Volume 25, Pages 28-35, 2017.

Hersbach, H., Bell, B., Berrisford, P., Hirahara, S., Horányi, A., Muñoz-Sabater, J., ... and Thépaut, J. N.: The ERA5 global reanalysis. Quarterly Journal of the Royal Meteorological Society, 146(730), 1999-2049. doi.org/10.1002/qj.3803, 2020.

Hieronymus, M., Hieronymus, J., and Hieronymus, F.: On the application of machine learning techniques to regression problems in sea level studies. Journal of Atmospheric and Oceanic Technology, 36(9), 1889-1902, 2019.

Horsburgh, K.J. and Wilson, C :Tide-surge interaction and its role in the distribution of surge residuals in the North Sea. Journal of geophysical research, Vol. 112, C08003, 2007.

Jacob, B., and EV Stanev, E. V.: Interactions between wind and tidally induced currents in coastal and shelf basins, Ocean Dynamics 67 (10), 1263-1281. doi.org/10.1007/s10236-017-1093-9, 2017.

Kramer, M. A.: Autoassociative neural networks. Computers & chemical engineering, 16(4), 313-328, 1992.

Kramer, M. A.: Nonlinear principal component analysis using autoassociative neural networks. AIChE journal, 37(2), 233-243, 1991.

Madec, G., Bourdallé-Badie, R., Bouttier, P. A., Bricaud, C., Bruciaferri, D., Calvert, D., ... and Vancoppenolle, M.: NEMO ocean engine. Notes du Pôle de modélisation de l'Institut Pierre-Simon Laplace (IPSL) (v3.6, Number 27), https://doi.org/10.5281/zenodo.1472492, 2017.

Madsen, K. S., Høyer, J. L., Fu, W., and Donlon, C.: Blending of satellite and tide gauge sea level observations and its assimilation in a storm surge model of the North Sea and Baltic Sea. Journal of Geophysical Research: Oceans, 120(9), 6405-6418, 2015.

Madsen, K. S., Høyer, J. L., Suursaar, Ü., She, J., and Knudsen, P.: Sea level trends and variability of the Baltic Sea from 2D statistical reconstruction and altimetry. Frontiers in Earth Science, 7, 243, 2019.

Mori, Y., Kuroda, M., and Makino, N.: Nonlinear principal component analysis and its applications, Springer, Singapore, 2016.

https://doi.org/10.5194/egusphere-2022-539
Preprint. Discussion started: 29 June 2022

Nieves, V., Radin, C., and Camps-Valls, G.: Predicting regional coastal sea level changes with machine learning. Scientific Reports, 11(1), 1-6, 2021.

O'Dea, E. J., Arnold, A. K., Edwards, K. P., Furner, R., Holt, J. T., Hyder, P., Liu, H., Martin, M. J., Siddorn, J. R., Storkey, D., and While, J.: An operational ocean forecast system incorporating NEMO and SST data assimilation for the tidally driven European north-west shelf, J. Oper. Oceanogr., 5, 3–17, 2012.

Peeck, H. H., Proctor, R., and Brockmann, C.: Operational storm surge models for the North Sea. Continental Shelf Research, 2(4), 317-329, 1983.

Ponte, R. M., Carson, M., Cirano, M., Domingues, C. M., Jevrejeva, S., Marcos, M., ... and Zhang, X.: Towards comprehensive observing and modeling systems for monitoring and predicting regional to coastal sea level. Frontiers in Marine Science, 6, 437, 2019.

Prandi, P., Meyssignac, B., Ablain, M., Spada, G., Ribes, A., and Benveniste, J.: Local sea level trends, accelerations and uncertainties over 1993–2019. Scientific Data, 8(1), 1-12, 2021.

Proudman, J. and Doodson, A. T.: The principal constituent of the tides in the North Sea., Phil Trans. R. Soc. Lond. A244: 185-219, 1924.

Staneva, J., Alari, V., Breivik, Ø., Bidlot, J. R., and Mogensen, K.: Effects of wave-induced forcing on a circulation model of the North Sea. Ocean Dynamics, 67(1), 81-101, 2017.

Staneva, J., Grayek, S., Behrens, A., and Günther, H.: GCOAST: Skill assessments of coupling wave and circulation models (NEMO-WAM). In Journal of Physics: Conference Series (Vol. 1730, No. 1, p. 012071). IOP Publishing, 2021.

Tayel, M. and Oumeraci, H.:A Hybrid Approach Using Hydrodynamic Modeling and Artificial Neural Networks for Extreme Storm Surge Prediction, Coastal Engineering Journal, 57:1, 1540004-36, 2015.

Thomson, Sir William: XVI. On gravitational oscillations of rotating water, The London, Edinburgh, and Dublin Philosophical Magazine and Journal of Science, 10:60, 109-116, DOI: 10.1080/14786448008626897, 1880.

https://doi.org/10.5194/egusphere-2022-539
Preprint. Discussion started: 29 June 2022

Tonani, M., Sykes, P., King, R. R., McConnell, N., Péquignet, A. C., O'Dea, E., ... and Siddorn, J.: The impact of a new high-resolution ocean model on the Met Office North-West European Shelf forecasting system. Ocean Science, 15(4), 1133-1158, 2019.

Wahl, T., Haigh, I. D., Woodworth, P. L., Albrecht, F., Dillingh, D., Jensen, J., ... & Wöppelmann, G.: Observed mean sea level changes around the North Sea coastline from 1800 to present. Earth-Science Reviews, 124, 51-67, 2013.

Wenzel, M., and Schröter, J.: Reconstruction of regional mean sea level anomalies from tide gauges using neural networks, J. Geophys. Res., 115, C08013, 2010.

Yang, L., Jin, T., Gao, X., Wen, H., Schöne, T., Xiao, M., and Huang, H.: Sea Level Fusion of Satellite Altimetry and Tide Gauge Data by Deep Learning in the Mediterranean Sea. Remote Sensing, 13(5), 908, 2021.

Zhang, Z., Stanev, E.V., and Grayek, S.: Reconstruction of the basin-wide sea level variability in the north sea using coastal data and generative adversarial networks. J. Geophys. Res. Oceans. 125, e2020JC016402, doi:10.1029/2020JC016402, 2020.